Available online at www.sciencedirect.com
SCIENCE DIRECT®
Computational Materials Science 35 (2006) 327–331
COMPUTATIONAL MATERIALS SCIENCE
www.elsevier.com/locate/commatsci

Vlasov simulations of electron dynamics in metallic nanostructures

G. Manfredi *, P.-A. Hervieux

IPCMS-GONLO, 23 rue du Loess, F-67034 Strasbourg, France

Received 24 April 2004; accepted 13 September 2004

Abstract

The ultrafast electron dynamics in metallic nanoparticles and thin metal films can be investigated using a semiclassical model based on self-consistent Vlasov–Poisson simulations. Here, we present an 'Eulerian' code that solves the Vlasov equation on a regular phase-space mesh. Eulerian codes possess several remarkable advantages over standard test-particle techniques: (i) they display a very low level of numerical noise; (ii) they are accurate even in regions of low electronic density; (iii) and, most importantly for nanosized objects, they preserve the fermionic character of the electron distribution at all times. Numerical examples are provided to illustrate the potential applications of this method to the study of electron transport in metallic nanostructures.
© 2005 Elsevier B.V. All rights reserved.

Keywords: Ultrafast electron dynamics; Nanoparticles; Thin metal films; Vlasov codes

1. Introduction

It is nowadays possible, by means of ultrafast spectroscopy techniques, to assess the femtosecond dynamics of an electron gas confined in metallic thin films [1–4] or nanoparticles [5,6], so that theoretical predictions can be directly compared to experimental measurements. In order to model and interpret such experimental results, ab-initio methods can hardly be employed, as they involve prohibitive computational times. A possible alternative relies on the use of microscopic kinetic methods, originally developed in nuclear and plasma physics, and applied more recently to metal clusters [7]. In these models, the valence electrons are assimilated to an inhomogeneous electron plasma. The quantum electron dynamics can be described in phase-space by the Wigner equation, coupled self-consistently to the Poisson equation. In the semiclassical limit, this Wigner–Poisson system reduces to the Vlasov–Poisson equations.

The numerical resolution of the Vlasov equation is usually performed with particle-in-cell (PIC) methods, which approximate the distribution function by a finite number of test particles [7]. However, the numerical noise inherent to this method is too large to allow a precise description of the distribution function in phase-space. Further, due to the finite number of particles used, PIC methods inevitably introduce some amount of random noise in the Vlasov dynamics, which drives the system towards classical Maxwell–Boltzmann thermalization. Therefore, the fermionic character of the electrons is not preserved during time evolution, which constitutes a major drawback for any PIC method.

On the contrary, Eulerian codes [8–12] rely on the resolution of the Vlasov equation on a regular mesh on the phase-space (x,v). They generally achieve finer resolution and display better convergence and stability properties than the corresponding PIC codes. In this work, we shall illustrate the good properties of a recently developed Eulerian scheme [11], which is capable of preserving the fermionic character of the electron

* Corresponding author. Tel.: +33 3 88 10 71 14.
E-mail address: Giovanni.Manfredi@ipcms.u-strasbg.fr (G. Manfredi).

0927-0256/$ - see front matter © 2005 Elsevier B.V. All rights reserved.
doi:10.1016/j.commatsci.2004.09.058

distribution *exactly and for all times*. Thanks to this numerical technique, we have been able to obtain clean and meaningful information on the electron dynamics in a metallic nanostructure.

2. Model

For simplicity, we shall only consider one-dimensional (1D) situations, although the numerical technique can easily be extended to higher dimensions. The electron dynamics is governed by the 1D Vlasov equation

$$\frac{\partial f_e}{\partial t} + v\frac{\partial f_e}{\partial x} + \frac{e}{m_e}\frac{\partial \phi}{\partial x}\frac{\partial f_e}{\partial v} = 0, \tag{1}$$

where $f_e(x, v, t)$ represents the electron distribution function in phase-space, and $e > 0$ and m_e are the electron charge and mass respectively. The electrostatic potential $\phi(x)$ is given self-consistently by Poisson's equation

$$\frac{\mathrm{d}^2\phi}{\mathrm{d}x^2} = \frac{e}{\varepsilon_0}[n_e(x) - n_i(x)], \tag{2}$$

with $n_e = \int f_e \,\mathrm{d}v$. The ions are supposed to be motionless and described by a density profile $n_i(x) = n_0[1 + \exp((|x| - L/2)/\sigma_i)]^{-1}$, where n_0 is the ion density of the bulk metal, σ_i a diffuseness parameter [7], and L is the spatial extension of the ion density. The above model (1) and (2) can be viewed as the classical limit of the fully quantum Wigner–Poisson system.

As an initial condition for Eqs. (1) and (2), we use the ground state calculated semiclassically using a Thomas-Fermi-like approach. The electron distribution is represented by a Fermi–Dirac (FD) function with finite temperature T_e

$$f_e^{\mathrm{FD}}(x, v) = n_0\left[1 + \exp\left(\frac{m_e v^2 - 2e\phi(x)}{2T_e}\right)\right]^{-1} \tag{3}$$

Note that the chemical potential is implicitly included in the arbitrary additive constant of the electric potential $\phi(x)$. By plugging the above FD distribution into Poisson's Eq. (2), we obtain a nonlinear equation for ϕ that can be solved by an iterative method to obtain the self-consistent potential ϕ and then the corresponding ground state distribution from Eq. (3).

The above Vlasov–Poisson equations represent a useful model to study the electron dynamics in nanosized objects such as metallic nanoparticles and thin metal films. The model is semiclassical in the sense that it includes the Fermi–Dirac statistics of the ground state, but neglects the quantum character of the electron dynamics. In order to take the latter into account, one should turn to the Wigner equation, which is the fully quantum analogue of the Vlasov equation. We are currently developing an Eulerian codes for the Wigner equation [13] in order to compare the present results with those obtained with a fully quantum model.

Returning to the present Vlasov–Poisson model, the main challenge is now to implement an accurate numerical technique that solves the time-dependent Vlasov equation. In particular, it is important that the numerical scheme preserves the fermionic character of the electron distribution, so that Pauli's exclusion principle is not violated. Note that the Vlasov equation *does* satisfy the exclusion principle, because of the conservation of phase-space volume in time (Liouville's theorem). However, numerical schemes do not necessarily preserve this property. The rest of this paper will be devoted to the presentation of a numerical technique for the Vlasov equation that, besides being stable and accurate, automatically satisfies this crucial physical property.

3. Eulerian Vlasov codes

The Vlasov equation is usually solved numerically by means of particle-in-cell (PIC) techniques. The basic idea is to represent the distribution function as a sum of delta functions:

$$f_e(x, v, t) = \sum_{j=1}^{N} w_j \delta(x - x_j(t))\delta(v - v_j(t)), \tag{4}$$

where the w_j are constant weights, and the positions x_j and velocities v_j of the N test-particles obey the equations of motion (characteristics of the Vlasov equation): $\dot{x}_j = v_j$ and $\dot{v}_j = -eE(x_j)/m_e$. The electric field $E = -\partial\phi/\partial x$ is computed by projecting the particle density on a spatial mesh and then solving Poisson's equation. For applications to degenerate electron plasmas, this method presents at least two drawbacks: (i) In the initial state the particles are loaded at random, so that a statistical noise is introduced, which will pollute the simulation results at all subsequent times. Statistical noise is proportional to $N^{-1/2}$, and is therefore difficult to eliminate by simply increasing the number of particles; (ii) Most importantly, PIC methods violate the exclusion principle, so that the initial FD quickly relaxes to a Maxwell–Boltzmann distribution (this relaxation is caused by the very same statistical noise mentioned above).

For semiclassical Vlasov simulations, Pauli's exclusion principle can be written in the following form: $f_e(x, v, t) \leqslant f_e(x, v, t = 0)$, where $f_e(x, v, t = 0)$ is the ground state FD distribution. In mathematical language, this means that the distribution function must respect a 'maximum principle' (and also a minimum principle, since obviously $f_e \geqslant 0$): this is guaranteed by the properties of the Vlasov equation, but generally not satisfied by PIC codes. The accuracy of PIC simulations can be somewhat improved by using finite-size particles (i.e. replacing the Dirac deltas in Eq. (4) with smoother

functions) [14] or by introducing ad-hoc collision operators [15]. Nevertheless, Maxwell–Boltzmann thermalization is still observed after some time. In addition, these corrections make it difficult to separate the collisionless Vlasov dynamics from the effect of such ad-hoc terms.

Eulerian methods [8] do not suffer from these drawbacks and should therefore be a useful tool for the simulation of nanoscale metallic objects, for which the electrons are highly degenerate. They are based on the resolution of the Vlasov equation on a regular mesh covering the entire phase-space (both position and velocity co-ordinates), which makes them somewhat more costly than PIC codes in terms of memory storage and computing time. The main advantage of Eulerian codes is that good accuracy is guaranteed even in regions of feeble electron density, where the statistical noise of a PIC code would be most prominent. The timestepping technique is based on a splitting algorithm [8], which amounts to solving separately the free-streaming term

$$\frac{\partial f_e}{\partial t} + v\frac{\partial f_e}{\partial x} = 0, \tag{5}$$

and the acceleration term

$$\frac{\partial f_e}{\partial t} - \frac{eE}{m_e}\frac{\partial f_e}{\partial v} = 0 \tag{6}$$

in the Vlasov Eq. (1). The solution from time t_n to time t_{n+1} can thus be obtained in three steps, corresponding to the solution of the free-streaming term (5) over half a time step, then the solution of the acceleration term (6) over a full time step, and finally again the free-streaming term (5) over half a time step:

$$f_e^{\star}(x,v) = f_e(x - v\Delta t/2, v, t_n) \tag{7}$$

$$f_e^{\star\star}(x,v) = f_e^{\star}(x, v + eE\Delta t/m_e) \tag{8}$$

$$f_e(x,v,t_{n+1}) = f_e^{\star\star}(x - v\Delta t/2, v) \tag{9}$$

where $f_e^{\star}$ and $f_e^{\star\star}$ denote intermediate solutions. Poisson's Eq. (2) is solved just before Eq. (8) to provide the electric field. Using the above symmetric scheme, the method is second order accurate in Δt.

We note that each term (7)–(9) gives rise to a constant shift in either position or velocity space. In their numerical implementation, these shifts require the interpolation of the distribution function in phase-space, which can be performed according to different schemes (cubic splines, finite volumes, fast Fourier transforms, ...). However, not all interpolation schemes will satisfy the exclusion principle. Here, we employ a numerical technique based on a finite-volume technique, in which the electron distribution is assimilated to a phase-space 'fluid' [9]. The scheme performs a detailed balance of the fluid entering and leaving each phase-space cell: in this way, the total mass $\iint f_e \,\mathrm{d}x\,\mathrm{d}v$ is conserved exactly (except, of course, for particles lost at the boundaries). This method has recently been upgraded by Filbet et al. [11] by introducing a slope corrector that prevents the distribution function from exceeding its initial maximum level (and from developing spurious negative values), while still conserving the total mass. With this correction, the model is able to preserve the fermionic nature of the electron distribution *exactly and for all times*.

4. Simulation results

In order to illustrate the potential applications of Eulerian Vlasov codes to the study of the electron dynamics in metallic nanostructures, we have performed several simulations in 1D slab geometry. A 1D geometry can actually have realistic applications to the electron dynamics in a thin metal film [16], as the film can be assumed to be infinite in the directions parallel to its surface. In all runs, time is normalized in units of the inverse plasmon frequency ω_{pe}^{-1}, velocity in units of the Fermi speed v_F, and length in units of $L_F = v_F/\omega_{pe}$. The slab thickness is taken to be $L = 40L_F$ and the diffuseness parameter in the ion density is $\sigma_i = 0.5\ L_F$. The initial electron temperature is $T_e = 0.1\ T_F$. The typical number of phase-space mesh points used in a simulation is $N_x = 5000$ and $N_v = 300$, with a time step $\omega_{pe}\Delta t = 0.05$.

First, the stability properties of the code have been tested by preparing the system in its ground state and letting it evolve self-consistently without any perturbation. By definition, the ground state is a stationary solution of the Vlasov–Poisson system and should remain stable under the time evolution. However, PIC codes show a rather quick deterioration of the Fermi–Dirac ground state, which relaxes to a Boltzmann distribution in a few (≈13) electron plasmon cycles [14,15]. With our Eulerian code, no departure from the Fermi–Dirac equilibrium can be detected for times as long as $\omega_{pe}t = 600$, corresponding to almost 100 plasmon cycles. The initial and final energy distributions $F(E)$ (obtained by integrating f_e over different energy surfaces) are shown in Fig. 1, and are almost indistinguishable on the scale of the figure. Further, during the evolution, the total energy is conserved with a relative error less than 3×10^{-6}. Such remarkable stability could not have been achieved with a PIC code.

Subsequently, in order to excite the electron dynamics, we have perturbed the electron ground-state distribution by shifting it in velocity space of a fixed quantity $\delta v = 0.06\, v_F$. In this way, an amount of energy $E^*/E_F = n_0 L(\delta v/v_F)^2$ is injected into the system in the form of kinetic energy of the center of mass of the electron population. After applying such perturbation, the electron cloud is left to evolve under the action of the self-consistent electric potential. The electron relaxation is studied by following the time history of several energy

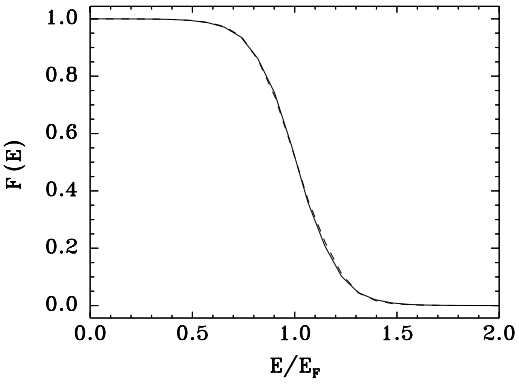

Fig. 1. Energy distribution at $t = 0$ (solid line) and $\omega_{pe}t = 600$ (dashed line) for an unperturbed Fermi–Dirac equilibrium.

quantities. The total energy of the electron gas is given by: $E_{\rm tot} = E_{\rm kin} + E_{\rm pot}$. The kinetic energy can further be split into three parts: (i) the kinetic energy of the center of mass: $E_{\rm cm} = \frac{1}{2}\int \frac{j_e^2(x)}{n_e(x)}\,{\rm d}x$ (where $j_e = \int v f_e\,{\rm d}v$ is the electron current); (ii) the Thomas-Fermi energy (energy of the equivalent zero-temperature state with same density), which in 1D reads as: $E_{\rm TF} = \frac{1}{6}\int n_e(x)^3\,{\rm d}x$; and (iii) the thermal energy: $E_{\rm th} = E_{\rm kin} - E_{\rm cm} - E_{\rm TF}$.

The evolution of such energy quantities is plotted in Fig. 2. The center-of-mass kinetic energy displays an oscillatory behavior at the plasmon frequency and decays down to a negligible value in a relatively short time ($\omega_{pe}t \simeq 100$). At the same time, the thermal energy rises of about $0.13\,E_{\rm F}$, which is very close to the value of the injected center-of-mass energy $E^* = 0.144\,E_{\rm F}$. The remaining part of E^* goes into the potential energy, which readjusts itself to a value slightly larger than that of the ground state. The Thomas-Fermi energy (not shown in figure) is almost unchanged during the entire run. It appears, therefore, that the center-of-mass energy is converted into thermal energy of the electron population. At the end of the run, the electrons have relaxed to

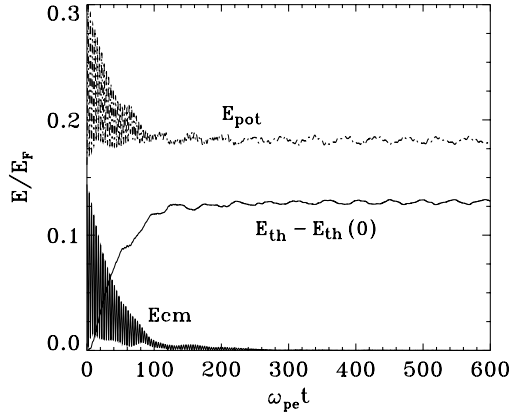

Fig. 2. Time evolution of the thermal, potential and center-of-mass energies (normalized to $E_{\rm F}$). The initial value of the thermal energy $E_{\rm th}(0) \simeq 0.4$ has been subtracted for clarity.

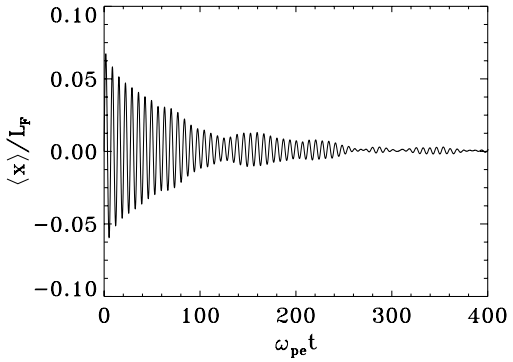

Fig. 3. Time evolution of the electron dipole.

a new quasi-stationary state characterized by a larger thermal energy (and therefore larger temperature) and an electric energy compatible with such a high temperature state. The evolution of the electron dipole $\langle x\rangle = \iint f_e x\,{\rm d}x\,{\rm d}v$ (Fig. 3) confirms that the motion of the center of mass of the electron distribution is gradually damped. The observed oscillations occur at the electron plasma frequency, as expected.

This picture is in agreement with the evolution of the energy distribution, shown in Fig. 4. The final distribution is indeed close to a Fermi–Dirac function characterized by a temperature higher than that of the ground state. We point out that this quasi-thermalization process is driven by purely mean-field effects, as no electron-electron collisions are taken into account in the model. Note that the exclusion principle is still satisfied even for this perturbed simulation (i.e. nowhere is the value $f_e = 1$ exceeded). The total energy is conserved with a relative error less than 2×10^{-4}.

Further, the fine resolution obtained with the Eulerian code allows us to follow the microscopic electron dynamics in the relevant phase-space, as illustrated in Fig. 5. It is clear from this figure (see, in particular, $\omega_{pe}t = 150$) that only electrons located near the Fermi surface play a significant role in the thermalization

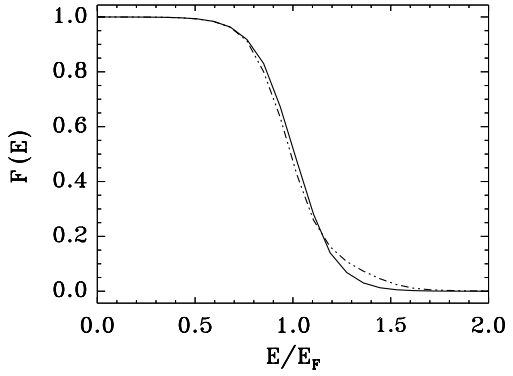

Fig. 4. Energy distribution at $t = 0$ (solid line) and $\omega_{pe}t = 600$ (dashed line). The initial Fermi–Dirac equilibrium was perturbed with $\delta v = 0.06 v_{\rm F}$.

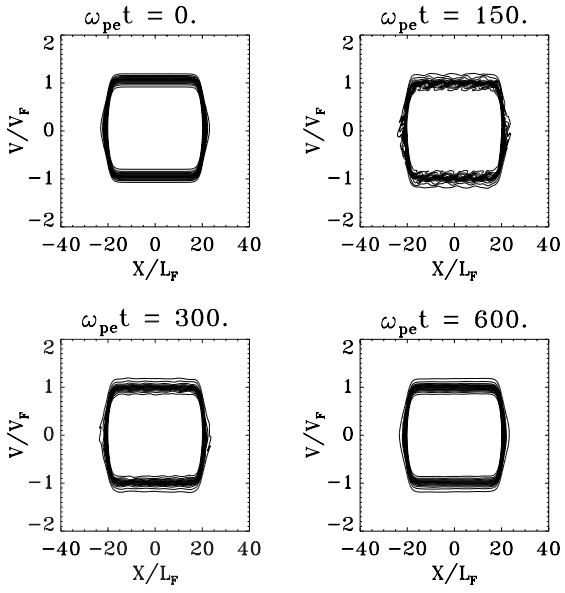

Fig. 5. Contour plots of the electron distribution function in phase-space at different times.

process. The initial perturbation propagates at a speed close to the Fermi velocity, so that the thermalization process appears to be of a *ballistic* rather than diffusive nature. This is in agreement with experimental results obtained with thin gold films [1,2].

5. Conclusion

In this work, we have presented a numerical method for the solution of the Vlasov equation that is particularly well adapted to the study of degenerate electron plasmas. The method is stable and accurate, and is capable of preserving the fermionic character of the electron distribution exactly. Numerical evidence has been presented in order to illustrate the good properties of such Eulerian codes. The numerical results have allowed us to describe with high accuracy the semiclassical electron dynamics and thermalization in a typical metallic nanostructure.

Although only 1D examples were reported for the sake of simplicity, the code can be easily extended to more spatial dimensions. Indeed, Eulerian codes are based on a splitting algorithm that treats each phase-space direction independently. Adding more dimensions would just increase the number of steps in the time-stepping algorithm (7)–(9).

Several extension of this work are possible and currently under way. The classical ion dynamics [16] can easily be added through an additional ion Vlasov equation. Further, it should be possible to include a collision integral (of the Ühling-Uhlenbeck type) that accounts for electron–electron collisions. As the Eulerian technique treats the collisionless (mean-field) dynamics with great accuracy, the effect of electron–electron collisions could then be studied without being polluted by spurious "numerical collisions" that are unavoidable with PIC codes.

Acknowledgements

We thank P. Bertrand and J.-Y. Bigot for helpful discussions, and F. Huot for assistance with the numerical calculations.

References

[1] S.D. Brorson, J.G. Fujimoto, E.P. Ippen, Phys. Rev. Lett. 59 (1987) 1962.
[2] C. Suárez, W.E. Bron, T. Juhasz, Phys. Rev. Lett. 75 (1995) 4536.
[3] G.L. Eesley, Phys. Rev. Lett. 51 (1983) 2140.
[4] C.-K. Sun, F. Vallée, L.H. Acioli, E.P. Ippen, J.G. Fujimoto, Phys. Rev. B 50 (1994) 15337.
[5] J.-Y. Bigot, V. Halté, J.-C. Merle, A. Daunois, Chem. Phys. 251 (2000) 181.
[6] M. Nisoli, S. Stagira, S. De Silvestri, A. Stella, P. Tognini, P. Cheyssac, R. Kofman, Phys. Rev. Lett. 78 (1997) 3575.
[7] F. Calvayrac, P.-G. Reinhard, E. Suraud, C. Ullrich, Phys. Rep. 337 (2000) 493.
[8] C.Z. Cheng, G. Knorr, J. Comput. Phys. 22 (1976) 330.
[9] E. Fijalkow, Comp. Phys. Comm. 116 (1999) 319.
[10] G. Manfredi, M. Shoucri, M.R. Feix, P. Bertrand, E. Fijalkow, A. Ghizzo, J. Comput. Phys. 121 (1995) 298.
[11] F. Filbet, E. Sonnendrucker, P. Bertrand, J. Comput. Phys. 172 (2001) 166.
[12] T.D. Arber, R.G.L. Vann, J. Comput. Phys. 180 (2002) 339.
[13] N. Suh, M.R. Feix, P. Bertrand, J. Comput. Phys. 94 (1991) 403.
[14] A. Domps, A.-S. Krepper, V. Savalli, P.-G. Reinhard, E. Suraud, Ann. Phys. (Leipz.) 6 (1997) 468.
[15] A. Domps, P.-G. Reinhard, E. Suraud, Ann. Phys. (N.Y.) 260 (1997) 171.
[16] G. Manfredi, P.-A. Hervieux, Phys. Rev. B 70 (2004) 201402 (R).